Chinese Journal of
POLYMER SCIENCE

ARTICLE

https://doi.org/10.1007/s10118-018-2020-3
Chinese J. Polym. Sci. 2018, 36, 514–520

Effect of Chain Extender on Hydrogen Bond and Microphase Structure of Biodegradable Thermoplastic Polyurethanes

Wen-Kai Liu, Yun Zhao, Rong Wang, Feng Luo, Jian-Shu Li, Jie-Hua Li*, and Hong Tan*

College of Polymer Science and Engineering, State Key Laboratory of Polymer Materials Engineering, Sichuan University, Chengdu 610065, China

Abstract Thermomechanical properties of polyurethanes (PUs) strongly depend on the molecular interactions and microphase structure. In this work, two chain extenders with different ratios, flexile 1,4-butanediol (BDO) and branched trimethylolpropane mono allyl ether (TMPAE), are used to tune the molecular interactions and microphase structures of a series of biodegradable thermoplastic polyurethanes (TPUs). In TPUs, the biodegradable polycaprolactone (PCL, M_n of 2000) is used as soft segment while 1,6-diisocyanatohexane (HDI) and chain extenders are used as hard segment. Fourier transform infrared spectroscopy (FTIR), proton nuclear magnetic resonance spectroscppy (^{1}H-NMR), gel permeation chromatography (GPC), differential scanning calorimetry (DSC), dynamic mechanical analysis (DMA) and mechanical tests were performed to characterize the bulk structure and properties of TPUs. Compared with BDO, the steric bulk of TMPAE is larger. The increment of TMPAE can help to increase the hydrogen bond content, microphase separation, and the elastic modulus ratio (R), which would strongly affect the thermomechanical property of the TPUs. The results of this work verify the importance of the structure of chain extender on the properties of TPUs. It provides valuable information for further understanding the structure-property relationships of these polyurethanes.

Keywords Chain extender; Hydrogen bond; Crystallinity; Polyurethane

Citation: Liu, W. K.; Zhao Y.; Wang, R.; Luo, F.; Li, J. S.; Li, J. H.; Tan, H. Effect of Chain Extender on Hydrogen Bond and Microphase Structure of Biodegradable Thermoplastic Polyurethanes. Chinese J. Polym. Sci. 2018, 36(4), 514–520.

INTRODUCTION

Polyurethane (PU) has become one of the most rapidly developed biomaterials due to its excellent biocompatibility, good physical and mechanical properties[1–6]. With the development of novel types of implanting medical devices, thermoplastic polyurethane (TPU) with degradable and shape-memory property is gaining increasing attention from industry and academia[7–12]. Compared with traditional shape memory alloys, the shape memory polyurethanes (SMPUs) possess lower cost, lighter weight, a wider range of recovery temperature (−30 °C to 70 °C), more admirable processing ability and better shape recovery ability[13, 14]. The SMPU materials appear to contain two separated phases, comprised of soft and hard segments. The soft segments which are sensitive to heat serve as molecular switches and are responsible for the shape recovery. The hard segments fix the shape before melting, imparting the materials elasticity and stiffness.

Many studies have investigated the structure and mechanism of SMPUs induced by heat[10, 15–17]. Among them, poly(ε-caprolactone) (PCL) is bio-degradable, crystallizable and widely used for soft segment of PU[18–20]. The crystallization and phase behavior of PCL strongly affect the properties of PUs, especially the shape-memory property. Kim *et al.* reported their synthesized polyurethanes based on poly(ε-caprolactone) (PCL) diols, methylenebis(4-phenyl-isocyanate) (MDI) and 1,4-butanediol, in which PCL-diols had a number-average molecular weight (M_n) between 2000 and 8000. This work certified that the soft segment molecular weight strongly affected the mechanical properties and shape recovery behavior. The shape memory ability of PU with high PCL molecular weight (M_n = 8000) was better than that of PU with low PCL molecular weight (M_n = 2000). These results were interpreted in terms of soft segment-hard segment phase separation and soft segment crystallization[21, 22]. Also, Ping *et al.* prepared a series of segmented poly(ε-caprolactone) polyurethanes (PCLUs) with a significant shape-memory effect, and the M_n of PCL was 500−10000. They found that the crystals were the key point of the shape recovery during the deformation and fixation. The recovery stress came from the inner stress stored in the deformed specimen during deformation and crystallization. The switching temperature could be adjusted to the range of 37–42 °C by adjusting the molecular weight of the PCL diols and the hard-to-soft ratio[18]. Moreover, Li *et al.* investigated the relationship between the molecular structure in PCL-based polyurethane system and the shape memory effect. They found that the high crystallinity of the soft segment was a prerequisite for the segmented copolymers to demonstrate shape memory behavior[21]. The lower limit of PCL molecular weight to

* Corresponding authors: E-mail jiehua_li@scu.edu.cn (J.H.L)
E-mail hongtan@scu.edu.cn (H.T.)
Received June 19, 2017; Accepted August 11, 2017; Published online November 1, 2017

crystallize under the usual processing conditions was found in the M_n range of 2000–3000. Therefore, all the results indicated that the crystallization plays an important role in shape fixation in segmented PUs. On the other hand, the hard-segment content, the length of the soft segment, and the total molecular weight of the block copolymer also affect the crystallization behavior of the PCL soft segments including the crystallinity, crystallization rate, and physical mobility[23].

Hydrogen bonding is another interaction affecting the mechanical property and shape memory effect of PUs system. The microphase separation of the hard domains and soft domains allows the materials to possess better mechanical properties[24]. Yang *et al.* studied on the effects of moisture on the glass transition temperature and thermomechanical properties of SMPUs and found that the hydrogen bonding between N—H and C=O groups was weakened by the absorbed water. The water absorbed into the SMPU could be separated into free water and bound water. The bound water significantly reduced the glass transition temperature in an almost linear manner and had a significant influence on the uniaxial tensile behavior, while the effect of free water was negligible[15]. The hydrogen bonding also exists beyond the condition of water environment; during the programming and recovery states it still plays an important role to conform the shape memory behavior. As the hard segment consisting of isocyanate and chain extender can both serve as hydrogen bond acceptors (C=O and —O—) and donors (N—H), it is our interest to explore the effects of the structure of the chain extender on the properties of the PUs.

In this work, we seek to explore the variation trend of hydrogen bond from our biodegradable polyurethane system which is prepared based on PCL, 1,6-diisocyanatohexane (HDI), 1,4-butanediol (BDO) and trimethylolpropane mono allyl ether (TMPAE). Here, BDO is a normal flexible chain extender, while TMPAE is a functional chain extender. The TMPAE has an allyl group as well as an ethyl group. Functional branch or crosslinking can be imported by the allyl group. Also, the branched TMPAE possesses larger steric bulk and enlarges the repulsion from soft domains to hard domains compared with BDO. Mixed chain extenders with different ratios are expected to change the hydrogen bond and phase behavior between the soft and hard segments. Therefore, the effects of chain extenders on the structure and thermomechanical properties of the TPUs are investigated.

EXPERIMENTAL

Materials

PCL diols (Daicel Chemical Industries Ltd, Japan) with molecular weight (M_n) of 2000 were dried under vacuum condition at 100 °C for 2 h. 1,6-Diisocyanatohexane (98%, HDI) (Aldrich Chemical Company, USA) and 1,4-butanediol (BDO, Aldrich, 99.5%) were purified by vacuum distillation. *N*,*N*-dimethyl acetamide (DMAc, 99%, Kelong in Chengdu, China) was dehydrated with CaH_2 for 2 days, purified by vacuum distillation and then dehydrated with 4Å molecular sieves. Trimethylolpropane mono allyl ether (TMPAE) (Perstorp AB), dibutyltin dilaurate (DBTDL) and chloroform (containing 0.03 wt% tetramethylsilane) were used without further purification.

Synthesis of Thermoplastic Polyurethanes (TPUs)

The synthetic route of TPUs is shown in Scheme 1 and the feed ratios are listed in Table 1. The synthesis method was modified according to our earlier work[25]. Briefly, quantitative PCL was added into a 250 mL three-necked round flask and was dried at vacuum under a reduced pressure at 100 °C for 2 h. Then DMAc, HDI and 0.02 wt% DBTDL were successively added into the flask for another 2 h at 80 °C under mechanical stirring to prepare pre-polymer. BDO was added into the reaction system for 1 h and then TMPAE was added for another 1 h at 60 °C, followed by polymerization at 80 °C for 2 h. Finally, it was heated up to 90 °C for the last 1 h. The solution was cooled to room temperature for 24 h. The polymer was precipitated in *n*-hexane. The lower sediment was transferred into a Teflon dish and dried at 60 °C for 24 h, and the cast film was further dried under 80 °C vacuum for 72 h. Here, the thermoplastic samples were referred to as "PU*x*". "PU" indicates the thermoplastic polyurethane; "*x*" indicates the percentage of TMPAE/(TMPAE + BDO). All the ratio of PCL:HDI:(TMPAE + BDO) = 1:3:2. To obtain low molecular weight of PU00L, a slight decrease of the content of HDI is performed (see Table 1).

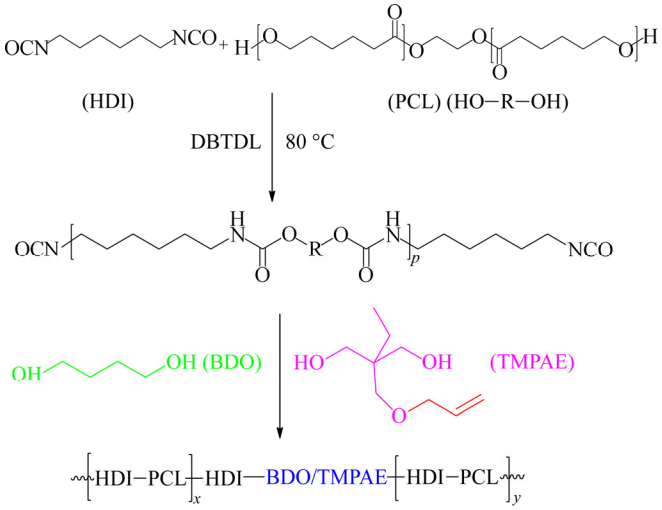

Scheme 1 Synthesis route of TPUs

Table 1 Composition, molecular weights and molecular weight distribution of the polyurethanes

Sample	Molar ratio PCL:HDI:BDO:TMPAE	$M_n \times 10^{-4}$ (g/mol)	$M_w \times 10^{-4}$ (g/mol)	M_w/M_n (PDI)
PU00L [a]	1:2.97:2:0	2.02	2.97	1.47
PU00H [b]	1:3:2:0	11.10	18.03	1.62
PU50	1:3:1:1	3.39	6.88	2.03
PU75	1:3:0.5:1.5	3.93	6.16	1.57
PU100	1:3:0:2	3.96	7.60	1.91

[a] Low molecular polyurethanes of PU00; [b] High molecular polyurethanes of PU00

Characterization

^{1}H-NMR analysis

The synthesis of PU was confirmed using a Bruker Advanced DPX-400 FT-NMR spectrometer (400 MHz) for polymer solutions in chloroform containing 0.03 wt% tetramethylsilane (TMS) as an internal standard.

https://doi.org/10.1007/s10118-018-2020-3

Gel permeation chromatography (GPC)

The molecular weights were measured using gel permeation chromatography (GPC) with DMF/LiBr as the mobile phase on the basis of a poly(methyl methacrylate) (PMMA) relative calibration. The test temperature was set at 40 °C. The flow rate of mobile phase was 1.0 mL/min. The calculated number-average molecular polymers are listed in Table 1.

Fourier transform infrared spectroscopy (FTIR)

Fourier transform infrared (FTIR) spectroscopy of TPUs was acquired using a Perkin-Elmer System 2000 FTIR spectrometer in the region of 400–4000 cm^{-1} at room temperature. Each sample was scanned 30 times at a resolution of 2 cm^{-1}, and the scan signals were averaged. The thicknesses of samples for FTIR were controlled so that the absorbance of the specimens was less than 1.

Differential scanning calorimetry measurement (DSC)

Thermal properties were measured by DSC experiments conducted on a TA Instruments Q1000 Differential Calorimeter at a programmed ramp of 10 K/min. The samples were subjected to two heating and cooling cycles between −100 and 100 °C, and the second heating and cooling cycle was recorded. DSC was used to determine the melting point (T_m) and crystallinity of PUs in the PCL phase was calculated according to the melting peak area of the DSC trace, assuming the perfect PCL crystal with a melting enthalpy of 0.14 kJ/g[23].

Mechanical properties analysis

Mechanical properties were determined by static tensile testing with an Instron 1121 instrument at a stretching rate of 50 mm/min at room temperature (23 °C). For each sample, at least three dumbbell-shaped specimens (effective dimensions of 20 mm × 4 mm × 1 mm) were prepared and tested. The ultimate strength and elongation at break of the polymers were obtained from the tensile tests and reported as average values.

Dynamic mechanical analysis (DMA)

Dynamic mechanical analysis (DMA) was measured using specimens with a size of 12 mm × 4 mm × 1 mm (length × width × thickness), and was carried out with a TA DMA-Q 800 at a heating rate of 3 K/min from −100 °C to 100 °C and a frequency of 1 Hz.

RESULTS AND DISCUSSION

Structure of TPUs by ^{1}H-NMR

To investigate the structure of the synthesized TPUs, Fig. 1 shows the ^{1}H-NMR spectra of PU00H, PU50, PU100 and the chain extender monomer TMPAE. By comparison of spectra of the TMPAE and PUs containing TMPAE, the typical resonance signals at 2.29–2.36 ppm (a, −CH_2−), 3.14–3.16 ppm (h, −CH_2−) and 5.13–5.26, 5.80–5.89 ppm (k, l, m, vinyl which indicates double bond content in the polymer) are found in the samples. The disappearance of −OH signal (3.65 ppm) of TMPAE and BDO indicates the full reaction of −OH groups with −NCO groups. For PU100, all the resonance signals including H-(a) at 2.29–2.36 ppm, H-(b, d) at 1.61–1.69 ppm, H-(c, i) at 1.33–1.49 ppm, H-(e) at 4.04–4.08 ppm, H-(h) at 3.14–3.15 ppm match with the corresponding protons, which indicates the successful synthesis of PU100. For PU50 and PU00H, each signal is associated with the corresponding proton of the proposed structure, verifying the successful preparation of PUs. Signals of H-(k", l", m", vinyl) at 4.82–5.12, 5.79–5.88 ppm from PU50 become weaker than those of PU100 as evidence that the vinyl from PU50 is half the amount of that from PU100. Meanwhile, there is no signal of H in vinyl group for PU00H because of the absence of TMPAE. According to the ^{1}H-NMR results, the TPUs with different ratios of TMPAE are synthesized successfully.

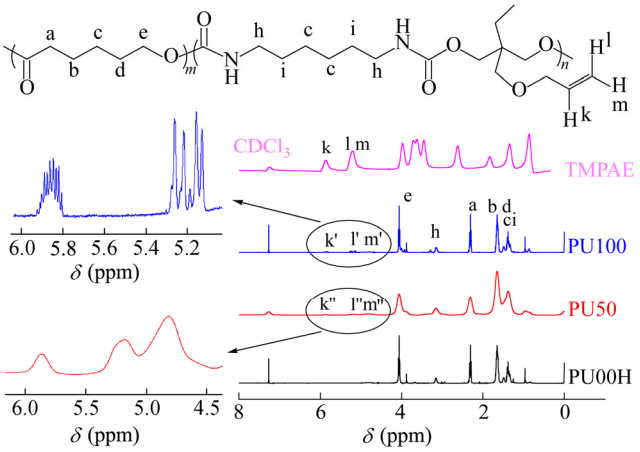

Fig. 1 ^{1}H-NMR spectra of TPUs

Structure and Hydrogen Bond Interaction of TPUs by FTIR Analysis

Figure 2 shows the FTIR spectra of TPUs. Peaks ranging in 3600–3200, 3000–2800, 1800–1600 and 1300–1000 cm^{-1} are attributed to the N−H, C−H, C=O and C−O−C vibration, respectively[26]. The peak around 1645 cm^{-1} is attributed to the C=C stretching of TMPAE group. Apparently, for all the samples, there are no peaks around 2273 cm^{-1}, which is attributed to the absorption of isocyanate (−NCO) groups, demonstrating that the −NCO group was reacted completely[27]. In TPUs, N−H acts as H donors, while C=O in urethane and PCL accepts H to form the hydrogen bond. With increasing the amount of TMPAE, the −NH stretching vibration at 3300–3400 cm^{-1} becomes broad, as shown in Fig. 2(b). It indicates a wide distribution of hydrogen bonds of −NH with urethane C=O and ester C=O in different configurations. Meanwhile, as the result of hydrogen bond interaction, the peak shape of C=O from 1800 cm^{-1} to 1600 cm^{-1} also shows a significant change with variation of TMPAE content, as shown in Fig. 2(c).

Hydrogen bond is a kind of inner force in polyurethane which is abundant and strong. Also, it is one of the most important driving force in shape memory materials. Therefore, the hydrogen bond content and micro-phase structure were analyzed by the FTIR spectra. The C=O signal in 1800–1600 cm^{-1} domain is usually used to investigate the hydrogen bond in polyurethane. Gaussian distribution curve-fitting is used to figure out the proportion of different kinds of carbonyl, as shown in Fig. 2(d). In this region, the hydrogen-bonded carbonyl absorption in PCL is at 1721 cm^{-1}, while the

https://doi.org/10.1007/s10118-018-2020-3

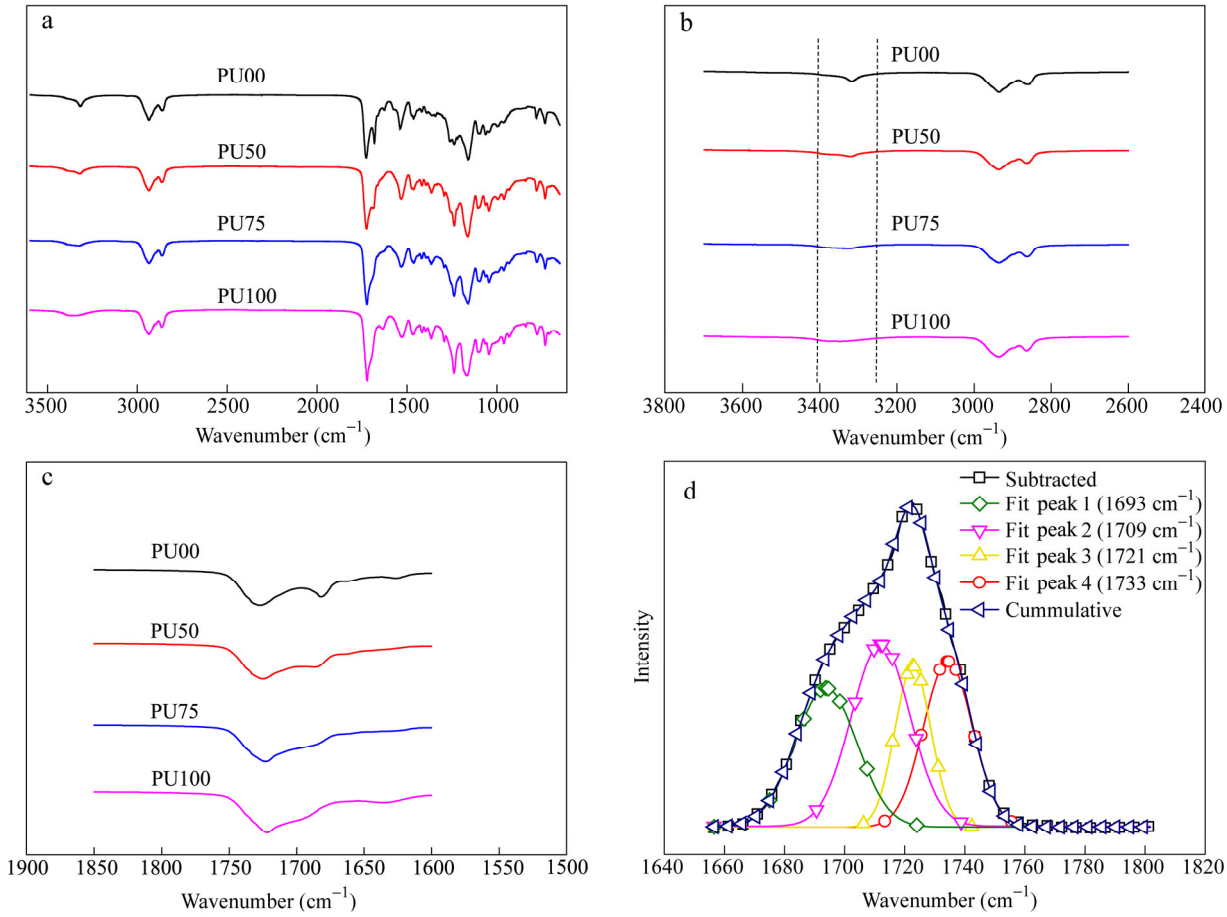

Fig. 2 FTIR spectra of TPUs: (a) the full spectra, (b) amplified regions from 2600 cm^{-1} to 3700 cm^{-1}, (c) amplified regions from 1600 cm^{-1} to 1850 cm^{-1}, (d) the typical split of carbonyl region between 1650 cm^{-1} and 1800 cm^{-1} of PU100

hydrogen-bonded carbonyl absorption in urethane linkage is at 1693 cm^{-1}. The other two peaks at 1733 and 1709 cm^{-1} belong to the free carbonyl stretching in PCL and in urethane linkage, respectively.

The contents of different kinds of carbonyl bond in the PCL and urethane are listed in Table 2. The hydrogen-bonded carbonyl ratio X of the three TPU samples with TMPAE slightly increases from 56.6% to 64.3% with the increase of TMPAE content, but they are obviously higher than that of TPUs with single BDO (about 46%). In detail, as listed in Table 2, with the increase of TMPAE, the hydrogen-bonded carbonyl in both the hard segment (1693 cm^{-1}) and soft segment (1721 cm^{-1}) gradually increase. The TMPAE has a larger steric hindrance compared with the other chain extender BDO. It might interrupt crystallization or chain packing, especially in the hard segments of TPUs. In this system, the situation seems more complex. The large steric hindrance of TMPAE presents another promoting effect of the phase separation between soft segments and hard segments. When the later effect becomes dominant, the phase separation will increase. Because both N—H and urethane C=O are in the hard segments, only the increasing aggregation of hard segments can cause the percentages of hydrogen-bonded C=O for urethane to increase. This phenomenon implies that TMPAE promotes the separation of the microphase which results in the increase of hydrogen-bonded C=O in urethane linkage from 20.6% (PU00H) to 26.9% (PU100). It is interesting that the hydrogen-bonded C=O between soft segments and hard segments represented by absorption at 1721 cm^{-1} in PCL also increases. This result indicates that the branched TMPAE would increase the chance to form hydrogen bond between soft segments and hard segments although the microphase separation between them is enhanced. The possible reason may be that the large steric hindrance of TMPAE enlarges the stacking space of hard segments so that the unbonded N—H at the interface can be easy to bond with C=O in soft segments. Therefore, the H-bonded C=O at 1721 cm^{-1} in PCL also increases.

Table 2 FTIR curve-fitting results of TPUs in carbonyl stretching region

Sample	Peak area (%)				$X^{\#}$ (%)
	1693 cm^{-1}	1709 cm^{-1}	1721 cm^{-1}	1733 cm^{-1}	
PU00L	15.36	28.55	30.86	25.22	46.22
PU00H	20.62	29.32	25.96	24.09	46.58
PU50	22.47	21.57	34.13	21.83	56.60
PU75	25.70	20.51	36.01	17.78	61.71
PU100	26.94	20.16	37.34	15.56	64.28

[#] The hydrogen-bonded carbonyl ratio (X) is calculated as follow:

$$X = \frac{\sum \text{Area(bonded)}}{\text{Area}(1600-1800\ cm^{-1})}$$

https://doi.org/10.1007/s10118-018-2020-3

Thermal Analysis of TPUs

To further understand the microphase structure, thermal properties of TPUs were characterized by differential scanning calorimetry (DSC). As shown in Fig. 3, the glass transition temperature (T_g) of all the samples appears at around −55 °C which could be attributed to the PCL soft segment. A series of large endothermic peaks can be observed in the reheating (10 K/min) scan in the range between 20 and 50 °C which indicates the melting temperature (T_m) of the soft segment. Between T_g and T_m, an exothermic peak appears for these TPUs with TMPAE. This peak would be a recrystallization peak for the precursory aligned PCL chains. The TMPAE has an allyl group as well as an ethyl group, which increases steric hindrance. The large steric hindrance of TMPAE in hard segments will enlarge the repulsion between soft segments and hard segments. During the phase separation, a shear force comes from the opposite movement of two phases. Thus, the PCL chains align along the shear force to form precursory orientation. When heating, the precursory aligned chains recrystallize preferentially. The glass transition temperature (T_g), the melting temperature (T_m), melting enthalpy (ΔH_m), and degree of crystallinity (X_c) calculated according to the standard melting enthalpy of PCL are listed in Table 3. Comparing PU00H with PU00L, with the molecular weight of polyurethanes increasing, the T_g (DSC) slightly increases and the T_m sharply drops from 38.01 °C to 16.59 °C. It indicates that the increasing of the degree of polymerization restricts the movement of soft segment and the crystallization of PCL is limited. Thus, PU00H shows the lowest degree of crystallinity among these TPUs. On the other hand, with the increasing ratio of TMPAE in the TPU, the recrystallization peak and the crystallinity of PCL in the TPUs increase. Especially, the crystallinity of PU100 is the highest at 22.2%. What is more, both the recrystallization temperature and melting temperature of PCL

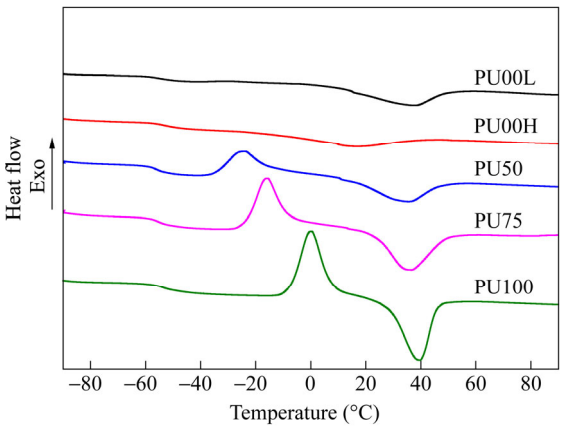

Fig. 3 DSC curves of TPUs

Table 3 Data of thermal properties for the TPUs from DSC

Sample	T_g (°C)	T_m (°C)	ΔH_m (J/g)	X_c (%)
PU00L	−56.06	38.01	10.45	7.5
PU00H	−53.3	16.59	5.92	4.2
PU50	−55.11	37.69	18.27	13.1
PU75	−53.44	37.89	26.36	18.8
PU100	−51.57	38.29	31.09	22.2

increase with increasing TMPAE. For TPU without TMPAE, a lower energy barrier of the nonpolar, uniform $-CH_2-$ exists in HDI and BDO part of PU. Meanwhile, C−C single bond can rotate at a low temperature. Thus, the hard segments formed by $-CH_2-$ and C−C deform easily and weakly separate from soft segments. Consequently, the TPU without TMPAE exhibits low microphase separation. The miscible behavior between hard segment and soft segment weakens the capability of precursory alignment of PCL chains. In contrast, the steric hindrance of the pendant groups of TMPAE in the hard segment causes a high energy barrier to deform and strong immiscibility with soft segments. In addition, TMPAE has fewer $-CH_2-$ units compared with BDO. When it is added in the TPU in a larger amount, the bulk of the hard segment increases and the movement becomes more difficult. When the TPU film is built at a low temperature, the pendant groups will hinder the chains entanglement between hard segments and soft segments, hence the microphase separation is promoted. Thanks to the promoting effect of microphase separation by TMPAE, the PCL chains in soft segment form more precursory aligned structure. During heating, the precursory aligned structure recrystallizes and the sample achieves high crystallinity. Therefore, the structure of chain extender affects the microphase behavior and results in the difference of hydrogen bonds content and crystallinity.

Dynamic Mechanical Analysis

It is known that the phase separation structure and the molecular chain interactions can be perfectly estimated by dynamic mechanical analysis (DMA). Therefore, the curves of TPUs by DMA are shown in Fig. 4 and the corresponding values of T_g (DMA), the storage modulus at T_g and (T_g + 50) °C, and dissipation factor of TPUs are listed in Table 4. tanδ peak location at the temperature axis indicates the T_g of TPU. Glassy state modulus (E'_g) roots in the elasticity of crystalline microphase and amorphous microphase, while rubbery state modulus (E'_r) originates from the entropy elasticity caused by microphase separation.

For PU00L and PU00H, at glassy state below −10 °C, E' of PU00H is higher than that of PU00L because of the high molecular weight of PU00H. Between −10 and 50 °C, E' of PU00L is slightly higher than that of PU00H because the degree of crystallinity of PU00L is higher compared with that of PU00H. At temperature above 50 °C, E'(PU00L) drops sharply because of the melting of crystalline PCL in PU00L. Obviously, PU00L has a poor performance in thermostability. In contrast, PU100H reaches a platform after a steady slide down. The better thermostability is a result of its high molecular weight.

For the TPUs with TMPAE, the hindrance of the pendant groups of TMPAE slows down the movement of molecular chain, thus the T_g shifts to higher temperature with increasing TMPAE content. In addition, the branched chain of TMPAE, comparing with BDO, is lack of flexibility, so molecular chains of the samples containing more TMPAE are blocked. Thus, the microphase separation is intensified. What is more, the tanδ peaks of TPUs with TMPAE are broader than those of TPUs without TMPAE. It is indicated that the molecular interactions between hard segment and soft segment in the

https://doi.org/10.1007/s10118-018-2020-3

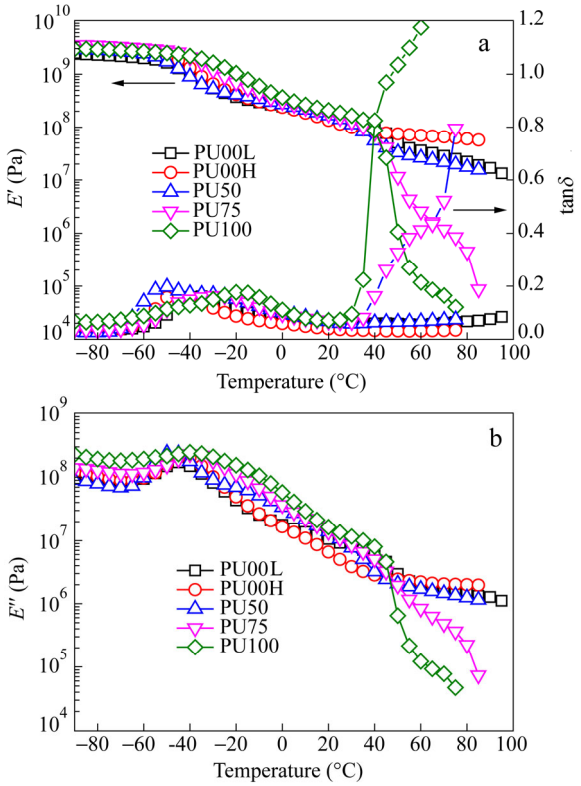

Fig. 4 The dynamic mechanical analysis of TPUs: (a) E' and tanδ versus temperature plots, (b) E'' versus temperature plots

Table 4 The glass transition temperature T_g (DMA), storage modulus at T_g, (T_g + 50) °C, dissipation factor (tanδ), and elastic modulus ratio R of TPUs

Sample	T_g (DMA) (°C)	E'_g (−80 °C) (MPa)	tanδ	E'_r (T_g + 50) (MPa)	R
PU00L	−37.7	2380	0.16	199	11.9
PU00H	−36.5	3053	0.17	165	18.5
PU50	−41.2	2924	0.20	220	13.3
PU75	−18.6	3519	0.16	119	29.6
PU100	−7.6	2938	0.18	56	52.5

TPUs with TMPAE are stronger than those in TPUs without TMPAE. That is to say, the TMPAE has strong effects on the formation of hydrogen bond between the two segments. This result agrees well with FTIR data. Considering the E' of TPUs with TMPAE, at −40~40 °C, E'(PU100) > E'(PU75) > E'(PU50). Also, it indicates that the molecular interaction in TPUs increases with increasing TMPAE content. At T > 40 °C, storage modulus experiences a sudden drop caused by the melting of PCL soft segment. At high temperature, the TPU samples are in rubbery state, and the branched TMPAE makes the space among the chains increase. Therefore, the E' of TPU with higher TMPAE content decreases sharply and E'(PU50) > E'(PU75) > E'(PU100). The elastic modulus ratio $R = E'_g/E'_r$ is one of the most important factors for shape memory property. The higher value the sample presents, the better shape memory property will be. That is, the low E'_r value makes materials change shape easily at high temperature, while the high E'_g value endows material with good deformation-existing abilities in low temperature environment. As shown in Table 4, R(PU100) > R(PU75) > R(PU50). The results indicate that the TPUs with higher TMPAE as well as higher crystallinity will possess better shape memory property. However, since the M_n of PCL is just 2000, as soft segments in this system, it is not enough to achieve high crystallinity to perform good shape memory[21]. Even for PU100 (X_c of 22.2%), the shape recovery ratio is below 50% tested by DMA. Since the TMPAE has an allyl group that can be further crosslinked, the crosslinked TPUs based on this system show excellent shape memory property which will be reported in our oncoming work.

Mechanical Analysis

The stress-strain curves of TPUs are shown in Fig. 5, and the average value of initial modulus, tensile strength and breaking strain are listed in Table 5. Crystalline polymer will present a cold drawing behavior when stretched at room temperature. The sample will neck partly and yield at a distinct drawing ratio. Thus, the stress-strain curves can reflect the crystallinity and microphase separation of TPU samples. In detail, PU00L shows the lowest tensile strength and minimum breaking strain. With increasing TMPAE in TPU, Young's modulus of TPUs gradually improves: E(PU50) = 61.4 MPa, E(PU75) = 99.9 MPa, E(PU100) = 159.8 MPa. Especially, PU75 and PU100 show distinctive yield points and necking because of their relatively high crystallinity and high degree of microphase separation. During stretching, PU75 and PU100 show plastic deformation. The molecular chains in crystalline phase will orientate along the stretch direction and untangle gradually. Such strain softening ability endows PU75 and PU100 with higher strain at break. In contrast, PU00L, PU00H and PU50 do not exhibit obvious yielding and necking. These samples show an elastic strain hardening behavior for amorphous polymer. The phenomena may be contributed by the relatively low microphase separation and the soft segments with low crystallinity.

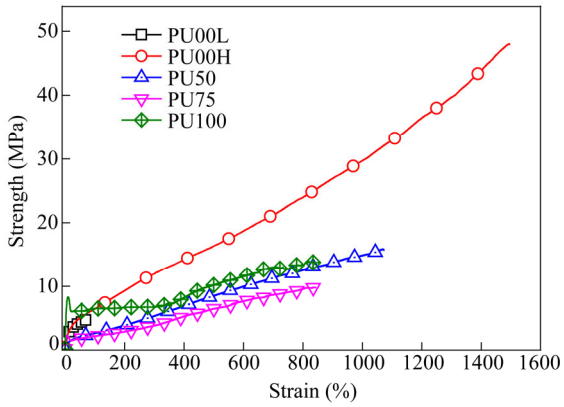

Fig. 5 Typical stress-strain curves for TPUs

Table 5 Mechanical properties of TPUs

Sample	Young's modulus (MPa)	Tensile strength (MPa)	Elongation at break (%)
PU00L	57.9 ± 6.5	4.2 ± 0.2	52.3 ± 4.0
PU00H	48.9 ± 3.6	48.4 ± 1.1	1520.2 ± 24.9
PU50	61.4 ± 3.4	10.6 ± 0.4	441.2 ± 20.5
PU75	99.9 ± 5.3	10.1 ± 0.3	902.5 ± 28.7
PU100	159.8 ± 8.5	13.3 ± 0.6	816.4 ± 37.3

https://doi.org/10.1007/s10118-018-2020-3

Combining the results of FTIR, DSC, DMA and tensile test, increasing TMPAE ratio in TPUs is in favor of microphase separation and forming hydrogen bonds. Because the TMPAE has unsaturated bonds, it can be further crosslinked or imported functional structure. The excellent shape memory behavior of the crosslinked TPUs based on this system will be reported in our oncoming work.

CONCLUSIONS

A series of TPUs based on PCL diol, HDI, BDO, TMPAE were synthesized by solution polymerization. The structures of the TPUs were confirmed by ^{1}H-NMR spectroscopy and FTIR spectrum. Gaussian distribution curve-fitting of FTIR and DSC results confirm that the chain extender TMPAE is positively related to the phase separation between soft segments and hard segments. The addition of branched TMPAE can promote the formation of hydrogen bonds and recrystallization in the PCL region. Thus, the PU100 with the highest TMPAE possesses the largest amount of hydrogen bond, the highest crystallinity, and the highest elastic modulus ratio. As both hydrogen bond interactions and crystallinity of TPU would affect its shape memory property, this work supplies some valuable information *via* the chain extender to tune the structure-property of shape memory polymers.

ACKNOWLEDGMENTS

This work was financially supported by the National Natural Science Foundation of China (No. 51573114), the National Science Fund for Distinguished Young Scholars of China (No. 51425305), and the Project of State Key Laboratory of Polymer Materials Engineering (Sichuan University) (No. SKLPME 2016-2-04).

REFERENCES

1 Cherng, J. Y.; Hou, T. Y.; Shih, M. F.; Talsma, H.; Hennink, W. E. Polyurethane-based drug delivery systems. Int. J. Pharm. 2013, 450(1), 145–162.
2 Zdrahala, R. J.; Zdrahala, I. J. Biomedical applications of polyurethanes: a review of past promises, present realities, and a vibrant future. J. Biomater. Appl. 1999, 14(1), 67–90.
3 Guelcher, S. A. Biodegradable polyurethanes: synthesis and applications in regenerative medicine. Tissue Eng., Part B: Reviews 2008, 14(1), 3–17.
4 Guan, J.; Fujimoto, K. L.; Sacks, M. S.; Wagner, W. R. Preparation and characterization of highly porous, biodegradable polyurethane scaffolds for soft tissue applications. Biomaterials 2005, 26(18), 3961–3971.
5 Song, N. J.; Jiang, X.; Li, J. H.; Pang, Y.; Li, J. S.; Tan, H.; Fu, Q. The degradation and biocompatibility of waterborne biodegradable polyurethanes for tissue engineering. Chinese J. Polym. Sci. 2013, 31(10), 1451–1462.
6 Ding, M. M.; Song, N. J.; He, X. L.; Li, J. H.; Zhou, L. J.; Tan, H.; Fu, Q.; Gu, Q. Toward the next-generation nanomedicines: design of multifunctional multiblock polyurethanes for effective cancer treatment. ACS Nano 2013, 7(3), 1918–1928.
7 Eceiza, A.; Martin, M.; de la Caba, K.; Kortaberria, G.; Gabilondo, N.; Corcuera, M.; Mondragon, I. Thermoplastic polyurethane elastomers based on polycarbonate diols with different soft segment molecular weight and chemical structure: mechanical and thermal properties. Polym. Eng. Sci. 2008, 48(2), 297–306.
8 Spontak, R. J.; Patel, N. P. Thermoplastic elastomers: fundamentals and applications. Curr. Opin. Colloid Interface Sci. 2000, 5(5), 333–340.
9 Wang, W. S.; Ping, P.; Yu, H. J.; Chen, X. S.; Jing, X. B. Synthesis and characterization of a novel biodegradable, thermoplastic polyurethane elastomer. J. Polym. Sci., Part A: Polym. Chem. 2010, 44(19), 5505–5512.
10 Huang, W.; Yang, B.; Zhao, Y.; Ding, Z; Huang, W. M.; Yang, B.; Zhao Y. Thermo-moisture responsive polyurethane shape-memory polymer and composites: a review. J. Mater. Chem. 2010, 20(17), 3367–3381.
11 Lai, S. M.; Lan, Y. C. Shape memory properties of melt-blended polylactic acid (PLA)/thermoplastic polyurethane (TPU) bio-based blends. J. Polym. Res. 2013, 20(5), 140–147.
12 Cui, B.; Wu, Q. Y.; Shen, L.; Yu, H. B. High performance bio-based polyurethane elastomers: effect of different soft and hard segments. Chinese J. Polym. Sci. 2016, 34(7), 901–909.
13 Guelcher, S. A.; Srinivasan, A.; Dumas, J. E.; Didier, J. E.; McBride, S.; Hollinger, J. O. Synthesis, mechanical properties, biocompatibility, and biodegradation of polyurethane networks from lysine polyisocyanates. Biomaterials 2008, 29(12), 1762–1775.
14 Lee, B. S.; Chun, B. C.; Chung, Y. C.; Sul, K. I.; Cho, J. W. Structure and thermomechanical properties of polyurethane block copolymers with shape memory effect. Macromolecules 2001, 34(18), 6431–6437.
15 Yang, B.; Huang, W. M.; Li, C.; Li, L. Effects of moisture on the thermomechanical properties of a polyurethane shape memory polymer. Polymer 2006, 47(4), 1348–1356.
16 Huang, W. M.; Yang, B.; An, L.; Li, C.; Chan, Y. Water-driven programmable polyurethane shape memory polymer: demonstration and mechanism. Appl. Phys. Lett. 2005, 86(11), 114105.
17 Altıntaş, Z.; Çakmakçı, E.; Kahraman, M. V.; Kayaman-Apohan, N. Thioether functional chain extender for thermoplastic polyurethanes. Chinese J. Polym. Sci. 2015, 33(6), 850–856.
18 Ping, P.; Wang, W. S.; Chen, X. S.; Jing, X. B. Poly(ε-caprolactone) polyurethane and its shape-memory property. Biomacromolecules 2005, 6(2), 587–592.
19 Zhou, L. J.; Yu, L. Q.; Ding, M. M.; Li, J. S.; Tan, H.; Wang, Z. G.; Fu, Q. Synthesis and characterization of pH-sensitive biodegradable polyurethane for potential drug delivery applications. Macromolecules 2011, 44(4), 857–864.
20 Rabani, G.; Luftmann, H.; Kraft, A. Synthesis and characterization of two shape-memory polymers containing short aramid hard segments and poly(ε-caprolactone) soft segments. Polymer 2006, 47(12), 4251–4260.
21 Li, F.; Zhang, X.; Hou, J.; Xu, M.; Luo, X.; Ma, D.; Kim, B. K. Studies on thermally stimulated shape memory effect of segmented polyurethanes. J. Appl. Polym. Sci. 1997, 64(8), 1511–1516.
22 Kim, B. K.; Lee, S. Y.; Xu, M. Polyurethanes having shape memory effects. Polymer 1996, 37(26), 5781–5793.
23 Bogdanov, B.; Toncheva, V.; Schacht, E.; Finelli, L.; Sarti, B.; Scandola, M. Physical properties of poly(ester-urethanes) prepared from different molar mass polycaprolactone-diols. Polymer 1999, 40(11), 3171–3182.
24 Chen, C. P.; Dai, S. A.; Chang, H. L.; Su, W. C.; Wu, T. M.; Jeng, R. J. Polyurethane elastomers through multi-hydrogen-bonded association of dendritic structures. Polymer 2005, 46(25), 11849–11857.
25 Jiang, X.; Li, J. H.; Ding, M. M.; Tan, H.; Ling, Q. Y.; Zhong, Y. P.; Fu, Q. Synthesis and degradation of nontoxic biodegradable waterborne polyurethanes elastomer with poly(ε-caprolactone) and poly(ethylene glycol) as soft segment. Eur. Polym. J. 2007, 43(5), 1838–1846.
26 Seymour, R.; Estes, G.; Cooper, S. Infrared studies of segmented polyurethan elastomers. I. Hydrogen bonding. Macromolecules 1970, 3(5), 579–583.
27 Su, T.; Wang, G. Y.; Xu, D. X.; Hu, C. P. Preparation and properties of waterborne poly-urethaneurea consisting of fluorinated siloxane units. J. Polym. Sci., Part A: Polym. Chem. 2006, 44(10), 3365–3373.